

Application of parametric resonance amplification in a single-crystal silicon micro-oscillator based mass sensor

Wenhua Zhang*, Kimberly L. Turner

Department of Mechanical and Environmental Engineering, University of California at Santa Barbara, Engineering II, R2355, Santa Barbara, CA 93106-5070, USA

Accepted 1 December 2004
Available online 3 March 2005

Abstract

A mass sensing concept based on parametric resonance amplification is proposed and experimentally investigated using a non-interdigitated comb-finger driven micro-oscillator. Mass change can be detected by measuring frequency shift at the boundary of the first order parametric resonance ‘tongue’. Both platinum deposition using focused ion beam (FIB) and water vapor desorption and absorption are used to change the mass of a prototype sensor. Due to the sharp transition in amplitude caused by parametric resonance, the sensitivity is 1–2 order of magnitude higher than the same oscillator working at Simple Harmonic Resonance (SHR) mode in air. Picogram (10^{-12} g) level mass change can be easily detected in the sensor with mass about 30 ng and resonance frequency less than 100 kHz. Damping effects and noise processes on sensor dynamics and sensing performance are also investigated and damping has no significant effect on sensor noise floor and sensitivity. Higher sensitivity is expected when the oscillator design is optimized and dimensions are scaled.
© 2005 Elsevier B.V. All rights reserved.

Keywords: Mass sensor; Chemical sensor; Parametric resonance; MEMS; Oscillator; Noise; Vapor detection

1. Introduction

As the technology of miniaturization develops rapidly, building micro/nanoscale oscillators becomes possible with much smaller mass and much higher frequencies than traditional mechanical oscillation systems. The concept of tracking resonant frequency (or phase) shifts of micro/nano-oscillators in the Simple Harmonic Resonance (SHR) mode to measure mass change has become a well-established technology in applications of chemical and biological sensing [1–8]. Since the fundamental resonant frequency of SHR depends on the mass and stiffness of the oscillator, mass change can cause resonance frequency to shift and so can be tracked by monitoring this frequency shift. Eqs. (1) and (2) describe the relationship between mass change and frequency shift. High sensitivity can be achieved in mass sensing using an oscillator with extremely small mass and

high resonant frequency, thus attracting much attention for sensor applications. In a micro-cantilever array, information on cantilever resonant frequency shifts can be used for recognition of a variety of chemical substances, including water, primary alcohols, and alkanes [2]. A single cell with an estimated mass of about 0.7 picogram (pg) has been detected based on a micro-cantilever oscillation measurement [3]. By creating even higher-frequency nanoscale oscillators (resonance frequency in MHz or GHz range), the ability of detecting femtograms (fg) or even attograms (ag) of mass change should be achievable [4–6,9–11].

$$f_0 = \frac{1}{2\pi} \sqrt{\frac{k}{m}} \quad (1)$$

$$\frac{dm}{m} = -2 \frac{df_0}{f_0} \quad (2)$$

Theoretically, any mass change in the sensing oscillator can cause a certain amount of frequency shift. If we can resolve this frequency shift, the corresponding mass change should

* Corresponding author. Tel.: +1 805 8937849; fax: +1 805 8938651.
E-mail address: whzh@engineering.ucsb.edu (W. Zhang).

be resolvable, as shown in Eqs. (1) and (2). However, the capability of frequency shift detection is governed by many factors, including readout circuitry, noise process, Quality factor of the oscillator, and others. Quality factor (Q), which denotes the sharpness of frequency response curve of Simple Harmonic Resonance, is one of the important factors that limit the sensitivity of the SHR based mass sensors. Micro/nano-oscillator with high Q can detect small mass changes because of the ability to resolve small frequency shift. Currently, silicon oscillators can achieve $Q \sim 10^3\text{--}10^5$ at low vacuum and low temperature. It is possible to detect mass changes in femtograms or even attograms. However, the applications of mass sensing in such environment are very limited, especially in chemical and biosensing, such as environmental monitoring and virus detection, where sensors are required to demonstrate high sensitivity in harsh environment. The sensitivity of mass detection can be dramatically lowered when operating in such environment as air or water, where Q is significantly lower, thus limiting sensitivity.

To improve the capability of frequency shift detection, significant effort has been put into improving Quality factor and frequency shift resolution, such as using feedback control to amplify the frequency response at resonance [12]. In our previous work, we have reported the conceptual basis of mass sensing using parametric resonance phenomenon [13–15]. In this mass sensing scheme, mass change is monitored by measuring frequency shift at the stability boundary of the first order parametric resonance ‘tongue’ [13–15]. The frequency transition at this boundary is very sharp [16], thereby making small frequency changes easily detectable and the frequency shift resolution high [14,15,17]. The sharpness of the boundary does not depend on the Quality factor (Q) [14,15,18,19]. Therefore, very small mass change can be detected in high-pressure environments, such as in air or even in water, where the sensitivity can be as high as in high vacuum. Of course this does not come for free, as there is more power required to create the oscillation in high-damping environments.

In this work, we present the first results investigating the feasibility of mass sensing based on parametric resonance phenomenon. This mass sensor is comprised of a single-crystal silicon micro-oscillator (Fig. 1), in which the backbone is supported by four-folded beams to provide recovery force for the oscillation and driven by a set of non-interdigitated comb-fingers using fringing-field electrostatic force [15,20]. Parametric resonance can be activated at certain frequencies because the non-interdigitated comb-fingers change the effective stiffness of the oscillator periodically in case an AC voltage signal is applied to actuate the oscillator [14]. Mass change can be determined by measuring the frequency change at the boundary of parametric resonance area [15]. To ‘create’ mass change to test the concept, a small volume of platinum (Pt) is deposited on the backbone using Focused Ion Beam (FIB). A similar micro-oscillator is designed as a reference in the same package to improve the sensitivity of mass sensing through common-mode

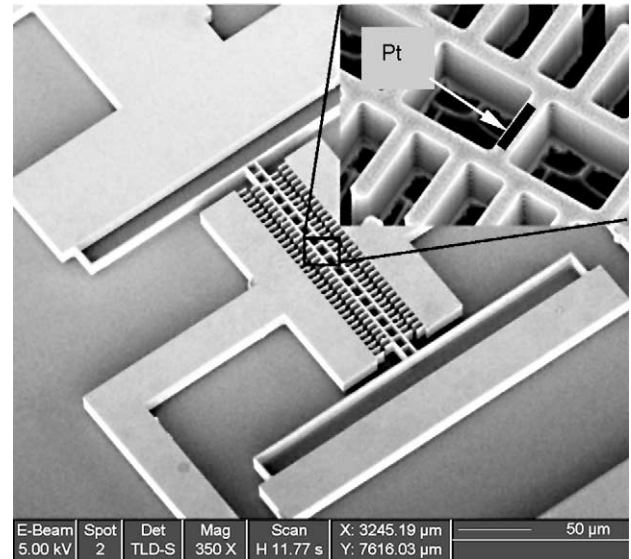


Fig. 1. A SEM picture of the prototype mass sensor. It has a backbone, four springs with folded beams to provide recovery force and one set of non-interdigitated comb-fingers to drive the oscillator. Platinum (Pt) deposition to change mass is schematically shown in this picture.

rejection. This preliminary device has sensitivity at the picogram (10^{-12} g) level when operating in air.

A noise process analysis has been completed to determine the effect of noise on the device sensitivity [15,21]. Because of the nonlinear dynamics nature of parametric resonance, the noise mechanism differs from normal Simple Harmonic Resonance based mass sensors. In this analysis, we consider thermal noise, Brownian motion, and actuation voltage fluctuation. Both the experiment and the analysis show that Brownian motion is an important noise source of the prototype mass sensor in the mass sensing application of parametric resonance in air, in addition to temperature and humidity fluctuation.

The ultimate sensitivity of this conceptual mass sensor is studied by testing water vapor content change in air pressure environment [15]. Less than 1 pg of mass change in the oscillator has been detected. This sensing capability agrees well with noise analysis results considering Brownian motion effects. Future work on sensitivity improvement and application using this technology are discussed at the end of the paper.

2. Theory

In previous work, we have discussed the parametric resonance dynamics of a similar oscillator in detail [14,15,22]. The micro-oscillator, shown in Fig. 1, can be simplified as a mass–spring system with electrostatic force as the driving force. When electrical signal is applied on the non-interdigitated comb-fingers, the electrostatic force generated is dependent on the position of the oscillator [14,15,20]. In the experiments presented here, we use a square rooted AC

voltage signal $(V_A(1 + \cos 2\omega t)^{1/2})$ to isolate the parametric resonance from direct harmonic response [17]. The movement of the device is governed by the nonlinear Mathieu-Hill equation [14].

$$\frac{d^2x}{d\tau^2} + \alpha \frac{dx}{d\tau} + (\beta + 2\delta \cos 2\tau)x + (\delta_3 + \delta'_3 \cos 2\tau)x^3 = 0 \tag{3}$$

$$\text{Here } \alpha = \frac{2c}{m\omega}, \quad \beta = \frac{4(k_1 + r_1 V_A^2)}{m\omega^2}, \quad \delta = \frac{2r_1 V_A^2}{m\omega^2},$$

$$\delta_3 = \frac{4k_3 + 4r_3 V_A^2}{m\omega^2}, \quad \delta'_3 = \frac{4r_3 V_A^2}{m\omega^2}$$

where m , k_1 , and k_3 are the mass, linear and cubic mechanical stiffness of the oscillator respectively, c is the damping coefficient, r_1 and r_3 are linear and cubic “electrostatic stiffness” and $\tau = \omega t$ is a normalized time [14].

Fig. 2 schematically shows the dynamics of this nonlinear Mathieu equation in β - δ plane defined above [14]. According to dynamic characteristics, the β - δ plane can be divided into three areas. Area II inside the “tongue” is the resonance area of the first order parametric resonance with one non-trivial solution, while areas I and III are non-resonance area with one trivial solution in area I and one trivial solution plus one non-trivial solution in area III. The characteristics of solutions and phase plane in each area are schematically shown in Fig. 2 as well, where “S” means stable and “U” means unstable. Here, we only consider stable solution, since unstable one cannot be observed experimentally. The dynamics can be more easily

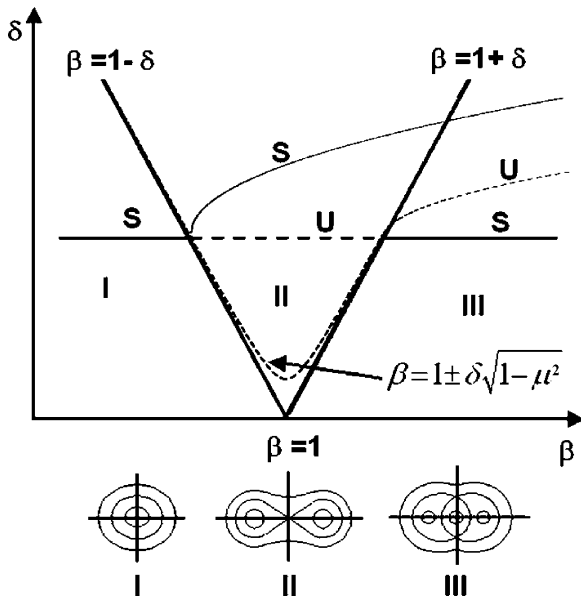


Fig. 2. Dynamic characteristics of nonlinear Mathieu-Hill equation in the β - δ plane. $\beta = 1 \pm \delta$ are the transition curves, which divide the β - δ plane into areas I, II and III. Note the damping effects on transition curves and how the positions of the stable (solid trace) and unstable (dashed trace) points vary as β and δ are varied quasi-statically. Phase planes in each area are shown as well.

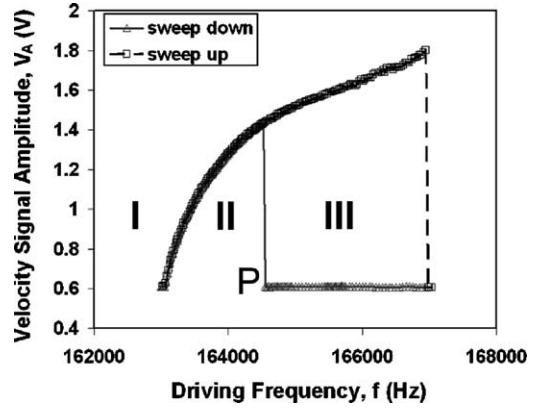


Fig. 3. Frequency response curves of the first order parametric resonance inside and outside of stability region. Area II is inside of “tongue”, as shown in Fig. 2, while I and III are outside. When sweep frequency down, resonance only happens in area II and there is completely no movement in areas I and III. A sharp jump happens at the right boundary of area II near point P.

understood in an experimental frequency response as shown in Fig. 3.

Fig. 3 shows the frequency response of parametric resonance inside resonance area (II) and outside of the resonance area (I and III) in device shown in Fig. 1. As the driving frequency goes up, the amplitude of the oscillator increases from the boundary between I and II and keeps increasing past the boundary between II and III. When sweeping down the driving frequency from area III, movement of the oscillator jumps to a large value from zero at the right boundary of area II and reduces in amplitude thereafter until it reaches zero at the left boundary. The frequency at the right boundary (point P), where the “jump” happens, is given by $f = (1/2\pi)\sqrt{(4k + 2r_1 V_A^2)/m}$, where k , m , V_A and r_1 are stiffness, mass, driving voltage amplitude, and the coefficient of electrostatic force, respectively. A small mass change (Δm) in the oscillator causes this “jump” frequency to shift (Δf). Therefore, by measuring the frequency shift, this mass change can be determined by $|\Delta m| \approx 2m(|\Delta f|/f_0)$.

The sensitivity of parametric resonance based mass sensor depends on the smallest frequency shift we can measure. Since the “jump” is a characteristic of nonlinear dynamics, where the characteristics of the dynamical equations change, the transition is very sharp and the change of frequency response is extremely ‘fast’ in the frequency domain. Therefore, the frequency at the boundary can be accurately defined. Very small frequency shift caused by mass change in the oscillator can be easily detected. In our previous work, a 0.001 Hz frequency shift (in 58,000 Hz) has been observed [17]. Damping affects the resonance boundary of the tongue, as shown in Fig. 2. At high damping, for example in air, actuation of parametric resonance requires more energy than at low pressure. However, the characteristics of dynamics keep the same as in low damping and the transition is still very sharp. Therefore, the frequency at the boundary can be still accurately found and damping has little

effect on the sensitivity of parametric resonance based mass sensors.

3. Devices and characterization

The micro-oscillators are fabricated from SOI wafer with highly doped device layer. The fabrication process is shown in Fig. 4. After patterning, a deep silicon etch process, DeepRIE-BOSCH process, is performed to form the micro structure, following by removal of photo resist left and wet chemical release of the buried silicon oxide layer to form the suspended MEMS structure. The thickness of the device is about 18 μm , which is defined by the thickness of the top device layer in the SOI wafer. The fabricated oscillator is a highly doped ($\rho \sim 0.01 \Omega\text{cm}$) single-crystal silicon device and electrically conductive.

Two similar devices have been made and tested here, named as device A and device B, so that one of them works as a mass sensor and the other as a reference sensor. The two devices have the same dimensions with the mass of backbone about 30 nanogram (ng), except that the springs of device A are of 1.5 μm wide and that of device B are of 2.0 μm wide, as shown in Fig. 1.

We characterize the fundamental dynamics characteristics using a laser vibrometer setup [23]. Since the devices move in-plane, a 45° mirror is made using FIB to guide detecting laser to the moving direction of the oscillator [23]. The natural frequencies of device A and B are about 49 and 83 kHz, respectively.

As we discussed earlier, damping plays a critical factor in SHR mode mass sensing. Fig. 5 shows frequency response curve of device A at different pressure, corresponding to different damping level. The sharpness of the frequency response curve decreases as pressure goes up. Fig. 6 shows Quality factor (Q) changes in different pressure, as expected [24]. The resonance frequency shift resolution at air pressure

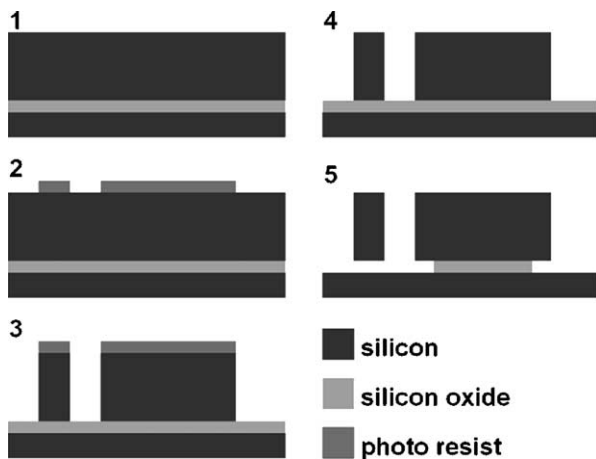


Fig. 4. Key steps in the SOI based bulk micro-machining process. (1) SOI wafer; (2) patterning; (3) DeepRIE etching; (4) photo resist removing, and (5) wet release etching of buried silicon oxide.

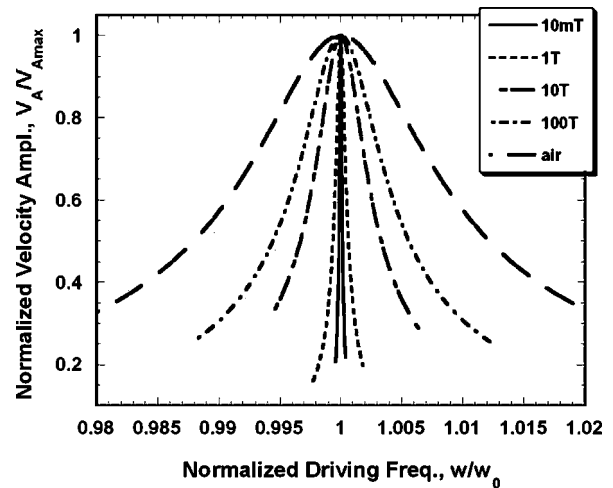


Fig. 5. Normalized frequency response curves of device A at different pressures.

is much lower than in low pressure, for example in 10 mTorr, where frequency resolution of the peak and mass sensitivity can decrease by 1–2 orders [10].

We also address the effects of damping on the behavior of parametric resonance and the potential effects on mass sensing application. The frequency response of parametric resonance is characterized at different pressure, as shown in Fig. 7. Here, we only sweep the driving frequency down, in which the frequency response is of interest in mass sensing. Parametric resonance boundary curves are also mapped as shown in Fig. 8.

As pressure changes, the frequency response curve of parametric resonance also varies. At high pressure, such as in air, the resonance area becomes smaller than low pressure and the minimum driving signal needed to actuate parametric resonance is larger. However the key characteristics in mass sensing application do not change, as shown in Fig. 7. The “jump” at the right boundary of the parametric resonance region still exists and is as sharp as in vacuum, as long as enough driving signal is applied. The sensitivity of mass sensing is not affected by testing environment pressure change.

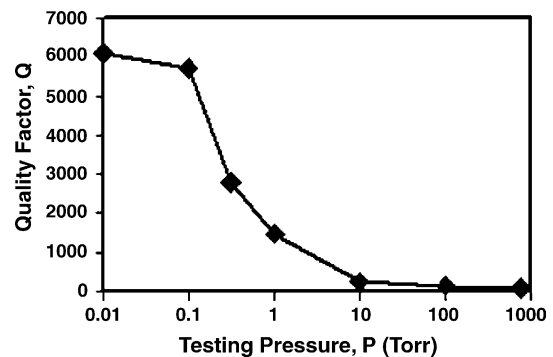


Fig. 6. Quality factor vs. pressure. Note that the Q factor changes as expected with operation pressure [24].

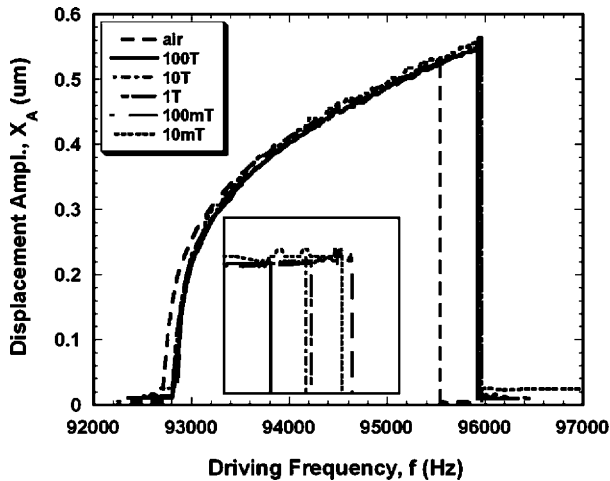


Fig. 7. Frequency response curves at different pressures. In this figure, only the sweeping down curves are shown.

4. Experiments

As a proof of concept, we first change the mass of the oscillator by attaching a set volume of platinum (Pt) on device A using FIB, as shown in Fig. 1. Three such mass changes, about 1, 4 and 0.4 μm^3 Pt deposition (corresponding to about 20, 80 and 8 pg), have been made. We record the frequency change at the right boundary of the first order parametric resonance area as discussed earlier before and after the deposition in air using laser vibrometry [23]. Meanwhile, device B works as a reference sensor and the frequency information is also recorded as a reference to environmental fluctuation, such as humidity and temperature.

The results of frequency shift in Pt deposition test are shown in Fig. 9. After each mass change, the “jump” frequency is recorded many times in a few days. The results are rectified according to frequency change in reference oscillator. The average frequency shift is about 36, 151 and 17 Hz, corresponding to 1, 4 and 0.4 μm^3 Pt deposition. Fig. 10 shows the relationship between frequency shift and volume of platinum deposition.

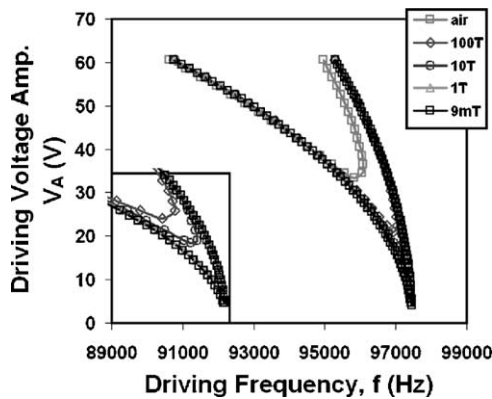


Fig. 8. Parametric resonance boundary curves for a variety of operating pressures.

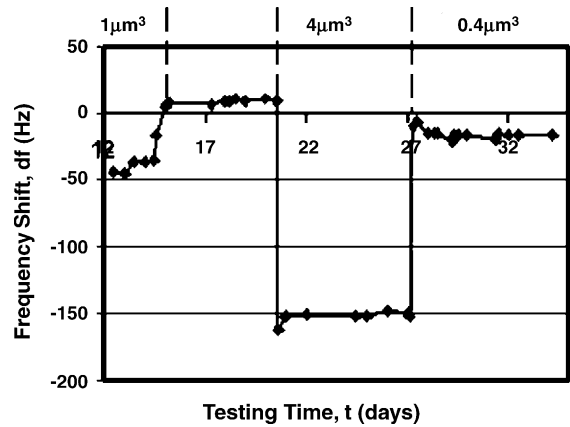


Fig. 9. Frequency shift in Pt deposition tests. Three mass changes have been made: 1, 4 and 0.4 μm^3 corresponding to about 20, 80 and 8 pg, respectively.

Good correlation is shown in the three tests between the volume of Pt deposition and “jump” frequency shift, which agrees very well with the analysis we discussed earlier that mass change is linearly dependent on frequency shift, $|\Delta m| \approx 2m(|\Delta f|/f_0)$, when mass change in the oscillator is small compared to the total mass. The minimum mass change here is about 8 pg.

Using platinum deposition to make mass change and measure frequency shift before and after Pt deposition has certain limitations to find the ultimate sensitivity of this prototype mass sensor. Since the tests are performed in many days, temperature and humidity fluctuation can contribute the frequency variation as well. As we can see from the results in Fig. 9, this frequency variation can be as big as 5–10 Hz, which is comparable to the frequency shift caused by Pt deposition of 8 pg.

To perform a more sensitive test and find the ultimate limit of mass sensing, the prototype mass sensor is also tested using adsorption of water vapor. Note that the oscillator is made of single-crystal silicon. After it is exposed in air, a thin layer of native silicon oxide grows on the surface. This native silicon oxide can absorb water molecules when it is exposed to environment with certain humidity [25]. Therefore, the mass of the device with native silicon oxide on the surface changes

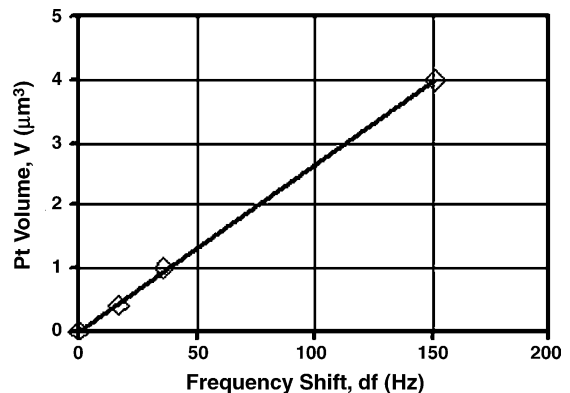


Fig. 10. Measured frequency shifts vs. the volume of Pt being deposited.

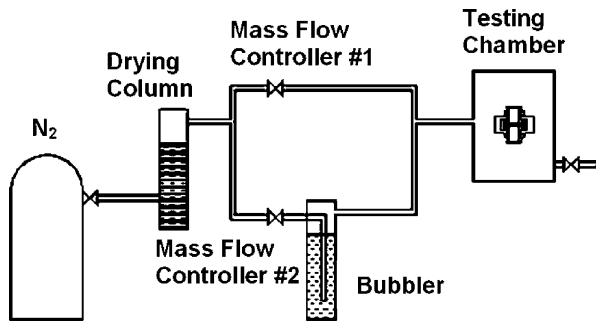


Fig. 11. Gas handling setup.

as humidity level varies. A gas handling setup is built to control the water vapor content in testing chamber, as shown in Fig. 11. A dry nitrogen gas flows through mass flow controller #1 directly to the testing chamber and another dry N_2 through mass flow controller #2 with water vapor from the water bubbler. By setting the flow rates of the two mass flow controllers, relative water content can be adjusted in the testing chamber. Here, we test the mass sensitivity of device B, since it has higher resonance frequency than device A and high sensitivity is expected. The frequency information of device B at the right boundary of the first order parametric resonance area is recorded, as water content in the testing chamber changes. By adjusting the water content, the resolution of frequency shift can be found and corresponding mass change can be determined. Since the test is performed in relative short time and humidity level is in controllable way, errors caused by temperature fluctuation are negligible.

Fig. 12 shows the results of frequency shift of device B as the relative water content is changed in air. When water content is switched on and off between 35 and 0% as shown in Fig. 12(a), the rate of frequency shift changes accordingly and the results shows good consistency between frequency shift and water vapor content change. The smallest controllable frequency shift we can measure using device B is less than 2 Hz, as shown in Fig. 12(b), which is equivalent to mass change of about 0.7 pg.

5. Noise processes and discussion

As with most micro-sensors [26–28], noise is an important issue in mass sensing using parametric resonance technology. The ability to detect ultra-fine frequency shift is compromised by noise processes in the oscillator. As we mentioned earlier, a 0.001 Hz or even smaller frequency shift has been observed [17]. However, in our current experiment, the frequency fluctuation is much larger than this value and the standard deviation of this frequency fluctuation we measured in these two oscillators is about 0.8 Hz at room temperature, as shown in Fig. 13(a). To analyze noise processes in mass sensing, we consider thermal noise, Brownian motion, and driving voltage fluctuation. Because the oscillator is driven by a pair of non-interdigitated comb-fingers the stiffness of the oscillator

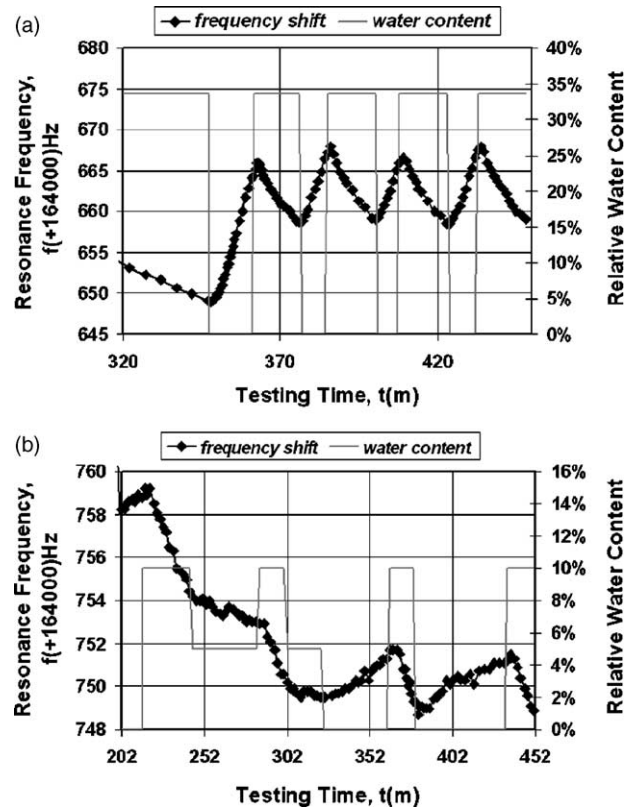


Fig. 12. Frequency shifts at the right side of the first parametric resonance area as adjusting water content in the testing chamber.

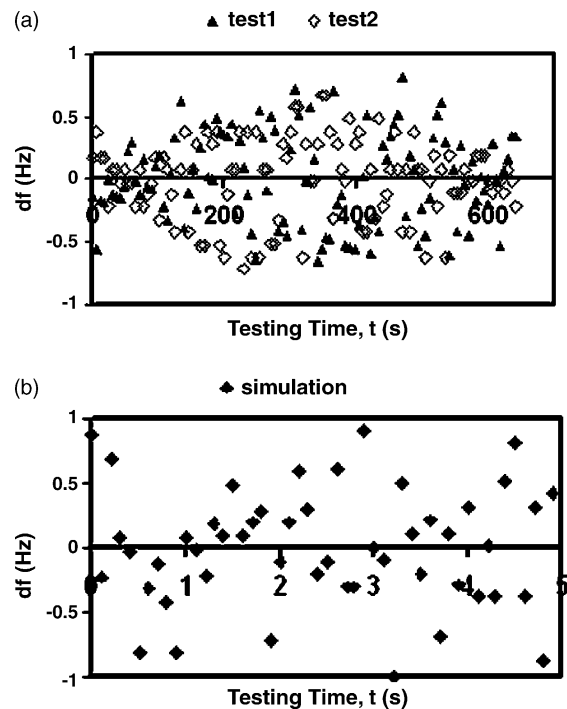


Fig. 13. Frequency variations at the boundary of parametric resonance area of (a) experiments and (b) simulation.

can be tuned by changing the driven electrical signal [20]. Therefore, any driven signal fluctuation can cause the resonance frequency and the boundary of parametric resonance to change. Both thermal noise in the testing circuit and signal source could bring about electrical signal variation and the frequency uncertainty.

Brownian motion can be another source of noise. According to dynamics of parametric resonance (see Fig. 2), the frequency at the boundary of resonance area depends on initial value before parametric resonance being excited. The variation of initial value affects the converging result in area III, as shown in the corresponding phase plane, and causes the frequency uncertainty at the stability boundary. In fact, Brownian motion of the oscillator can be treated as the initial value in the simulation from the view of dynamics.

To evaluate noise effects on frequency shift resolution and mass sensitivity, numerical simulation method is used to calculate the frequency fluctuation caused by thermal noise, Brownian motion, and driving voltage fluctuation. The results show that the frequency fluctuation caused by both thermal noise and driving voltage fluctuation is negligible compared to that of Brownian motion noise. One of the possible reasons is the effect of the nonlinearity of parametric resonance, which filters most of the noise energy from Johnson noise and driving voltage fluctuation in the actuation circuit. At room temperature, the standard deviation of Brownian motion is estimated about 0.5 \AA , which causes 0.7 Hz of frequency fluctuation according the simulation results, as shown in Fig. 13(b). The result agrees well with measured result in Fig. 13(a). Therefore, Brownian motion of oscillators is considered to be a main noise source in parametric resonance based mass sensing in the prototype mass sensor.

Certainly, there are other issues, which can be considered noise effects in mass sensing, such as frequency drift caused by humidity fluctuation and temperature fluctuation in the environment. We notice that this frequency drift can be larger than that caused by Brownian motion even with reference sensor when the test lasts days. However, by using an oscillator array and optimizing the design of sensors and reference sensors, this noise effect can be minimized in real-time mass detection.

As we mentioned earlier, damping effect is concerned since it affects the mass sensitivity of harmonic resonance mode mass sensor significantly. Here, we measured the frequency fluctuation level at the right boundary of parametric resonance region, as shown in Fig. 14. When pressure changes from 10 mTorr to air pressure, the standard deviation of frequency fluctuation is less than 0.5 Hz and shows no obvious pressure dependence. Therefore, the mass sensitivity considered to be hardly affected by damping and the sensor can achieve the same mass sensitivity level in air pressure as in vacuum.

The devices presented here are prototype mass sensors to test the concept of parametric resonance mass sensing, and are not yet at the limits of sensitivity or size. By tailoring the oscillator dimensions (for example, using cantilever geome-

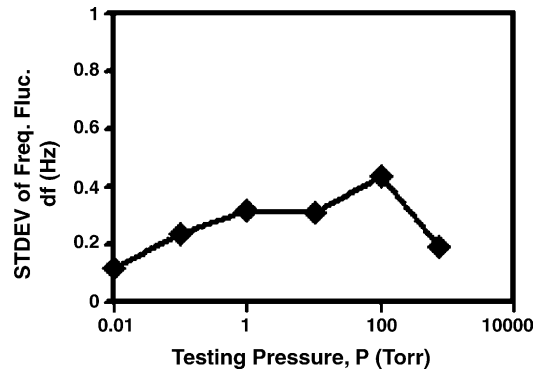


Fig. 14. Frequency fluctuations at the boundary of parametric resonance at different pressure.

try), increasing resonance frequency, or designing oscillator arrays, the sensitivity can be further improved, thus possibly extending their application to DNA, virus, and other analytes with mass in the order of attograms (ag). We calculated the noise level of device A with dimensions reduced by a factor of five. The equivalent mass resolution will be at femtogram (fg) level in air pressure. Now, many smaller micro/nano-oscillators have been made with higher frequencies, such as micro-cantilever and nanowire [29,30], and parametric resonance has been realized in these devices. Thus, significant improvement in cantilever based mass sensors based on parametric resonance is achievable, and currently underway.

6. Conclusions

Parametric resonance based mass sensor has been developed in this work. Because of damping effect, the sensitivity of SHR based mass sensor decrease dramatically in air. Using parametric resonance, the sensitivity can improve more than one order of magnitude. Damping has little effect on the sensing ability when operated in parametric resonance mode.

The measurement, taken in air, demonstrates that a prototype mass sensor based on parametric resonance can improve sensitivity 1–2 orders compared to the same sensor working in harmonic mode. The prototype mass sensors can detect mass changes at picogram (pg) level when operating in parametric resonance mode with mass of 30 ng and resonance frequency less than 100 kHz . The same sensitivity level can be achieved in air pressure as in vacuum when operating in SHR mode. The sensitivity can be further improved by optimizing the sensor design, such as using cantilever geometry, decreasing the mass of oscillator, and increasing resonance frequency.

References

- [1] T. Thundat, E.A. Wachter, S.L. Sharp, R.J. Warmack, Detection of mercury vapor using resonating micro-cantilevers, *Appl. Phys. Lett.* 66 (1995) 1695–1697.

- [2] F.M. Battiston, J.P. Ramseyer, H.P. Lang, M.K. Baller, C. Gerber, J.K. Gimzewski, E. Meyer, H.J. Guntherodt, A chemical sensor based on a microfabricated cantilever array with simultaneous resonance-frequency and bending readout, *Sens. Actuators B: Chem.* **B77** (2001) 122–131.
- [3] B. Ilic, D. Czaplewski, M. Zalalutdinov, H.G. Craighead, P. Neuzil, C. Campagnolo, C. Batt, Single cell detection with micromechanical oscillators, *AIP for American Vacuum Soc, J. Vacuum Sci. Technol. B* **19** (2001) 2825–2828.
- [4] N.V. Lavrik, P.G. Datskos, Femtogram mass detection using photothermally actuated nanomechanical resonators, *Appl. Phys. Lett.* **82** (2003) 2697–2699.
- [5] A. Gupta, D. Akin, R. Bashir, Single virus particle mass detection using microresonators with nanoscale thickness, *Appl. Phys. Lett.* **84** (2004) 1976–1978.
- [6] B. Ilic, H.G. Craighead, S. Krylov, W. Senaratne, C. Ober, P. Neuzil, Attogram detection using nanoelectromechanical oscillators, *J. Appl. Phys.* **95** (2004) 3694–3703.
- [7] T. Ono, L. Xinxin, H. Miyashita, M. Esashi, Mass sensing of adsorbed molecules in sub-picogram sample with ultrathin silicon resonator, *Rev. Sci. Instrum.* **74** (2003) 1240–1243.
- [8] H.P. Lang, R. Berger, F. Battiston, J.P. Ramseyer, E. Meyer, C. Andreoli, J. Brugger, P. Vettiger, M. Despont, T. Mezzacasa, L. Scandella, H.J. Guntherodt, C. Gerber, J.K. Gimzewski, A chemical sensor based on a micromechanical cantilever array for the identification of gases and vapors, *Appl. Phys. A* **66** (1998) S61–S64.
- [9] Z.J. Davis, G. Abadal, O. Kuhn, O. Hansen, F. Grey, A. Boisen, Fabrication and characterization of nanoresonating devices for mass detection, *J. Vac. Sci. Technol. B Microelectron. Nanometer Struct.* **18** (2000) 612–616.
- [10] K.L. Ekinci, Y.T. Yang, M.L. Roukes, Ultimate limits to inertial mass sensing based upon nanoelectromechanical systems, *J. Appl. Phys.* **95** (2004) 2682–2689.
- [11] X.M.H. Huang, C.A. Zorman, M. Mehregany, M.L. Roukes, Nanodevice motion at microwave frequencies, *Nature* **421** (2003) 496.
- [12] A. Mehta, S. Cherian, D. Hedden, T. Thundat, Manipulation and controlled amplification of Brownian motion of micro-cantilever sensors, *Appl. Phys. Lett.* **78** (2001) 1637–1639.
- [13] K.L. Turner, W. Zhang, Design and analysis of a dynamic MEM chemical sensor, in: *Proceedings of the 2001, American Control Conference*, vol. 1212, Arlington, VA, USA, 25–27 June, 2001, pp. 1214–1218.
- [14] W. Zhang, R. Baskaran, K.L. Turner, Effect of cubic nonlinearity on auto-parametrically amplified resonant MEMS mass sensor, *Sens. Actuators A, Phys.* **102** (1–2) (2002) 139–150.
- [15] W. Zhang, K.L. Turner, A mass sensor based on parametric resonance, in: *Hilton Head 2004: A Solid State Sensor, Actuator and Microsystems Workshop*, Hilton Head Island, South Carolina, June 6–10, 2004, p. 49.
- [16] K.L. Turner, S.A. Miller, P.G. Hartwell, N.C. Macdonald, S.H. Strogartz, S.G. Adams, Five parametric resonances in a microelectromechanical system, *Nature* **396** (1998) 149–152.
- [17] K.L. Turner, P.G. Hartwell, F.M. Bertsch, N.C. Macdonald, Parametric resonance in a microelectromechanical torsional oscillator, in: *ASME International Mechanical Engineering Congress and Exposition Proceedings of Microelectromechanical Systems (MEMS)*, Anaheim, CA, USA, 15–20 November, 1998, pp. 335–340.
- [18] A.H. Nayfeh, D.T. Mook, *Nonlinear Oscillations*, Wiley, New York, 1995, pp. 704.
- [19] M. Cartmell, *Introduction to Linear, Parametric, and Nonlinear Vibrations*, Chapman and Hall, London; New York, 1990, p. 242.
- [20] S.G. Adams, F.M. Bertsch, K.A. Shaw, N.C. Macdonald, Independent tuning of linear and nonlinear stiffness coefficients [actuators], *J. Microelectromech. Syst.* **7** (1998) 172–180.
- [21] W. Zhang, K.L. Turner, Noise analysis in parametric resonance based mass sensing, in: *ASME International Mechanical Engineering Congress and Exposition*, Anaheim, California, November 13–19, 2004.
- [22] W. Zhang, R. Baskaran, K.L. Turner, Tuning the dynamic behavior of parametric resonance in a micromechanical oscillator, *Appl. Phys. Lett.* **82** (2003) 130–132.
- [23] K.L. Turner, Multi-dimensional MEMS motion characterization using laser vibrometry, in: *Transducers'99 The 10th International conference on solid-state Sensors and Actuators*, Digest of Technical Papers, Sendai, Japan, 7–10 June, 1999, pp. 1144–1147.
- [24] J. Mertens, E. Finot, T. Thundat, A. Fabre, M.H. Nadal, V. Eyraud, E. Bourillot, Effects of temperature and pressure on micro-cantilever resonance response, *Ultramicroscopy* **97** (2003) 119–126.
- [25] H.P. Lang, M.K. Baller, F.M. Battiston, J. Fritz, R. Berger, J.P. Ramseyer, P. Fornaro, E. Meyer, H.J. Guntherodt, J. Brugger, U. Drechsler, H. Rothuizen, M. Despont, P. Vettiger, C. Gerber, J.K. Gimzewski, The nanomechanical NOSE, in: *Proceedings of 12th International Workshop on Micro Electro Mechanical Systems: MEMS*, Orlando, FL, USA, 17–21 January, 1999, pp. 9–13.
- [26] A.N. Cleland, M.L. Roukes, Fabrication of high frequency nanometer scale mechanical resonators from bulk Si crystals, *Appl. Phys. Lett.* **69** (1996) 2653–2655.
- [27] J.R. Vig, K. Yoonkee, Noise in microelectromechanical system resonators, *IEEE Trans. Ultrason. Ferroelect. Frequency Control* **46** (1999) 1558–1565.
- [28] T.B. Gabrielson, Mechanical-thermal noise in micromachined acoustic and vibration sensors, *IEEE Trans. Electron Devices* **40** (1993) 903–909.
- [29] Y. Min-Feng, G.J. Wagner, R.S. Ruoff, M.J. Dyer, Realization of parametric resonances in a nanowire mechanical system with nanomanipulation inside a scanning electron microscope, *Phys. Rev. B Condensed Matter* **66** (2002), 073406/073401–073404.
- [30] M. Napoli, R. Baskaran, K. Turner, B. Bamieh, Understanding mechanical domain parametric resonance in micro-cantilevers, in: *Proceedings IEEE Sixteenth Annual International Conference on Micro Electro Mechanical Systems*, Kyoto, Japan, 19–23 January, 2003, pp. 169–172.

Biographies

Wenhua Zhang received his B.S. in Naval Architecture and Ocean Engineering from Shanghai Jiao Tong University, his M.S. in Plasma Processing from Institute of Mechanics, Chinese Academy of Sciences, and his Ph.D. in Mechanical Engineering from University of California, Santa Barbara, where he is currently a postdoctoral researcher. Dr. Zhang's research interests include dynamics of micro/nano systems, sensor developments, micro/nano fabrication, and micro/nano devices modeling, testing and characterization. Dr. Zhang is a member of ASME, IEEE, and SEM.

Kimberly Turner received her B.S. in Mechanical Engineering from Michigan Technological University in 1994 and her Ph.D. in Theoretical & Applied Mechanics from Cornell University in 1999. She is currently an Associate Professor of Mechanical and Environmental Engineering at the University of California, Santa Barbara, CA where she has served on the faculty since 1999. Dr. Turner's research interests include nonlinear dynamics of micro/nanoscale systems, testing and characterization of MEMS devices, modeling of micro/nanoscale devices, and solid-state sensor development. Dr. Turner is a member of ASME, IEEE, SEM, AVS, and the Cornell Society of Engineers. She has received the NSF CAREER award, and the Varian Award from the AVS.